AIAA 81-1606R

Integral Rocket/Ramjet Propulsion—Flight Data Correlation and Analysis Techniques

Frank F. Webster*
Martin Marietta Corporation, Orlando Aerospace, Orlando, Fla.

The ASALM-PTV liquid fueled integral rocket/ramjet propulsion system was recently validated during seven successful flight tests. All program objectives were accomplished, including a correlation of flight and ground propulsion system data. All flight vehicles were extensively instrumented with pressure, temperature, and miscellaneous parameter measurements to evaluate the delivered propulsion performance characteristics. Several flight data analysis techniques were investigated to assess their reliability in determining delivered ramjet performance. The correlation of flight and ground test data was found to be excellent. The only region of significant deviation occurred during the initial seconds of ramjet operation due to the effects of booster residuals. This paper addresses PTV propulsion system flight test results, analysis techniques, and flight-to-ground data correlation.

Nomenclature

A_C = inlet capture area
$A_{1.7}$ = transport duct area
A_5 = nozzle throat area
A_6 = nozzle exit area
A_∞ = captured freestream area
C_F = nozzle thrust coefficient (sonic)
$C_{F_{id}}$ = nozzle thrust coefficient (expanded)
C^* = actual combustor characteristic velocity
C^*_{id} = ideal combustor characteristic velocity
D_{body} = body drag
D_{vane} = air vane drag
F/A = fuel-to-air ratio
g = gravity factor
m = vehicle mass
M_D = transport duct Mach number
P_{marg} = inlet supercritical pressure margin
$P_{T1'}$ = inlet face pitot pressure
$P_{T1.7}$ = transport duct total pressure
P_{T4} = combustor total pressure
$P_{T\infty}$ = freestream total pressure
P_1 = inlet face static pressure
$P_{1.7}$ = transport duct static pressure
P_3 = combustor forward dome pressure
P_4 = combustor static pressure
$P_{46.5}$ = inlet diffuser static pressure
P_∞ = freestream pressure
R = gas constant
S^*_a = air specific impulse
T_{gross} = gross ramburner thrust
T_{inlet} = inlet structure temperature
T_{net} = ramjet net thrust
T_{nozzle} = nozzle structure temperature
T_{T2} = inlet air total temperature
V_X = vehicle axial acceleration
V_∞ = freestream velocity
$\dot{W}_F$ = fuel flow rate
$\dot{W}_{1.7}$ = airflow rate in duct
$\dot{W}_2$ = airflow rate into combustor
α = angle of attack
γ = ratio of specific heats
ΔT_{id} = ideal combustion temperature rise
η_C = combustion efficiency
η_{noz} = nozzle efficiency

Presented as Paper 81-1606 at the AIAA/SAE/ASME 17th Joint Propulsion Conference, Colorado Springs, Colo., July 27-29, 1981; submitted Sept. 8, 1981; revision received Jan. 18, 1982.

*Staff Engineer, ASALM Propulsion Systems. Member AIAA.

Introduction

THE theoretical performance of the ramjet propulsion system is far better than either solid or liquid rocket motors. The liquid fueled ramjet is actually approaching its 70th birthday since its conception by Rene Lorin of France in 1913. Yet, in a relatively long development period, the ramjet has had considerable difficulty proving its worth. Table 1 summarizes the early U.S. ramjet missile programs which developed at least to a flight demonstration level. Although high speed, high altitude, and long ranges were attained, each of these missiles suffered from the common ailment of massive size for delivered range.

Interest in the ramjet abated after the ramjet development era in the 1940s and 1950s; however, it has recently been revived owing to five technological advances.

1) Tremendous advances in reducing the size and weight of guidance and warhead systems have decreased required missile size.

2) Delivered inlet and ramburner component efficiencies and fuel properties have improved considerably.

3) Structural materials are now available that can withstand the severe thermal/structural environment associated with high speed ramjets.

4) Ramburner thermal protection systems were devised to project the combustor case from the 4000 + °R gas temperature for long durations.

5) The advent of the integral rocket/ramjet (IRR) has resulted in greater packaging efficiencies for ramjets.

Solid propellant grain is packaged integrally within the ramjet combustion chamber in the IRR concept. This eliminates the need for tandem or strap-on solid rocket motors which are necessary to accelerate the ramjet to operational speed. The result is a considerable reduction in required missile size. The IRR technology was first demonstrated during the low altitude short-range missile (LASRM) program, but this missile had a limited operational envelope as shown in Fig. 1. The highly successful advanced low volume ramjet (ALVRJ) program extended the technology, but was still limited in capability.

Table 1. Early U.S. ramjet missile programs

Name	Type	Performance			Size		Status
		Mach	Altitude, kft	Design range. n.mi.	Length, ft	Weight, lb	
Navaho	Surf-surf	3.25	60	6300	95	290,000	Flight tested
Rigel	Surf-surf	2.00	60	600	47	25,000	Flight tested
Bomarc	Surf-air	2.9	120	400	44	16,000	Operational
Talos	Surf-air	2.5	80	80	33	7,800	Operational
Redhead/ Roadrunner	Drone	1.5	20	40	25	860	Operational
Typhon	Surf-air	4.0	100	400	28	20,000	Flight tested

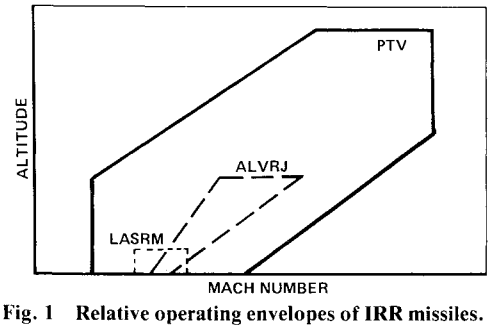

Fig. 1 Relative operating envelopes of IRR missiles.

The IRR technology was recently pushed to an advanced level of maturity during the propulsion technology validation (PTV) program. This contract was part of the Air Force Aeronautical Systems Division's technological development of the advanced strategic air-launched missile (ASALM). Figure 1 illustrates the PTV capability in relation to the other IRR configurations, with operation having been extended to high supersonic speeds at high altitudes. The advances in ramjet missile technology are evident in the PTV missile, which was designed in the same range category as Bomarc and Typhon, but with about one-eighth the launch weight.

After a ground test development and performance documentation program, seven missiles were flight tested over a broad range of conditions covering most of the design envelope. The IRR operated successfully during each of the flights.

Objectives

The PTV program had four primary objectives:

1) to demonstrate the technical maturity and performance capability of the liquid fueled IRR;

2) to evaluate the IRR performance characteristics in the dynamic environment that can only be accomplished in flight;

3) to conduct a performance correlation between flight test and ground test data; and

4) to update analytical tools for evaluating future IRR systems.

The first two objectives were accomplished during the seven flights by operating at a broad range of flight conditions covering the majority of the design operating envelope. Objectives 3 and 4 were accomplished through a comprehensive flight data analysis and flight-to-ground data correlation program.

An all too common tendency in today's development programs is that the amount of data evaluation is inversely proportional to the program's success. Detailed analysis of test data is often reserved for the investigation of failures. PTV is an exception to this trend. A comprehensive flight-to-ground data correlation program was conducted as a complement to the seven-out-of-seven successful flight tests. This performance evaluation program had five basic objectives:

1) to assess the delivered ramjet flight performance characteristics during both steady-state and transient conditions;

2) to correlate steady-state flight performance data with ground test results;

3) to assess flight performance evaluation techniques for an IRR system;

4) to evaluate the adequacy of the PTV ground performance documentation test program to predict flight performance; and

5) to update appropriate analytical models for use in evaluation of future IRR systems.

A summary of the flight performance results is included in this paper along with the flight-to-ground data correlation. The various techniques for computing flight performance are illustrated and evaluated. A summary of the ground test program is also presented along with an evaluation of the program's ability to adequately predict performance.

ASALM-PTV Propulsion System

The ASALM-PTV IRR propulsion system and flight test vehicle are illustrated in Fig. 2. The air induction system was comprised of a chin inlet, an underslung kidney-shaped air transport duct, and an S-shaped duct that translated the airflow to the combustor centerline. The combustor was a coaxial dump, sudden expansion configuration with a V-gutter flame-holder and an aerogrid mounted immediately in front of the dump plane. The Inconel 718 combustor was protected from the 4000+ °R combustion gases by a Dow-Corning DC93-104 thermal protection liner, while the ramjet nozzle used tape wrapped silica phenolic insulation. The booster propellant was cast integrally within the ramjet combustor. Since the booster needed a smaller nozzle than the ramjet owing to higher operating pressures, an ejectable nozzle was inserted within the ramjet nozzle. A frangible glass port cover was mounted in the combustor forward dome to complete the integral booster configuration.

The fuel management system (FMS) was operated pneumatically, using the pressure in the inlet transport duct as an airflow reference. The system was controlled by signals from the autopilot to vary the fuel-to-air (F/A) ratio between its 0.020 and 0.060 limits for speed control. An inlet pressure margin override control was physically present, but was disconnected prior to the start of the flight test program. The fuel expulsion system was an elastometric bladder pressurized by bleeding air from the transport duct.

Flight Test Program

The relative flight profiles for each of the seven PTV flights are summarized in Fig. 3. The IRR propulsion system operated successfully during each of the flights. Transition from rocket to ramjet was accomplished by each missile. Positive ramjet acceleration capability was demonstrated at each flight condition throughout each flight. Delivered propulsion system performance characteristics were close to prediction over the vast majority of the flight times.

There were only two significant missile system anomalies and both were related to contamination. A clogged pneumatic line to the FMS on flight 1 resulted in wide open fuel flow and constant acceleration until fuel depletion at a near hypersonic velocity. The missile structure broke up after fuel exhaustion

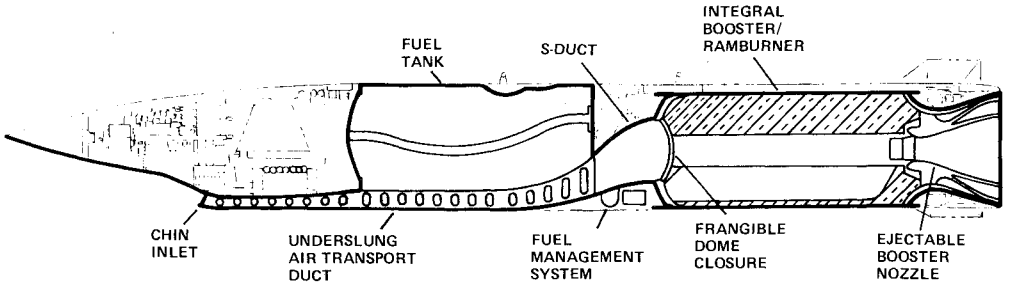

Fig. 2 ASALM-PTV propulsion system.

Table 2 Summary of fuel depletion flight times

Flight	Description	Flight time to fuel depletion, s: Preflight prediction	Actual	Deviation, %
4	Midaltitude launch Low altitude run-in High g turn	130.6	129.8	−0.6
5	Midaltitude launch Low altitude run-in Velocity excursions	138.3	136.3	−1.4
6	Low altitude launch Low altitude run-in Yaw turn	115.8	118.2	+2.1
7	Midaltitude launch High altitude cruise Powered dive	473.8	467.5	−1.3
		Average deviation		1.4

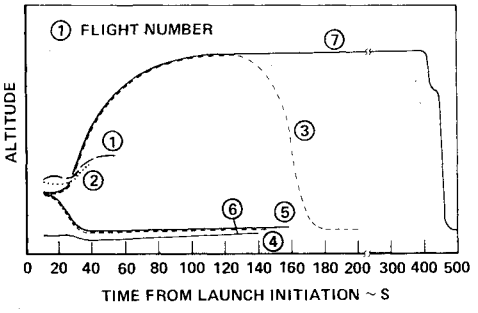

Fig. 3 Summary of PTV flight test profiles.

owing to the extreme thermal conditions. During flight 2, contamination in the hydraulic system resulted in the loss of air vane control and an early termination of flight. Flights 3-7 were 100% successful.

The PTV program goal was to demonstrate three primary trajectories:

1) a low altitude launch followed by at least 90 s of sustained cruise;

2) a split level trajectory consisting of a powered dive from high altitude with a pullout at low altitude; and

3) a long-range endurance trajectory consisting of at least 350 s while cruising at high supersonic speed at high altitude.

These three objectives were accomplished on flights 6, 3, and 7, respectively. The other trajectories were used to explore additional regions of the PTV operating envelope and to collect data for the flight-to-ground data correlation.

Flight Data Analysis Results

The propulsion system performance characteristics were in close agreement with predictions throughout each of the flights. This correlation applied both on an overall integrated level and on a point-by-point basis.

The ability to predict flight performance from the ground test program is best indicated by the overall flight duration. A comparison of actual flight times and preflight predictions for those flights progressing to fuel depletion is given in Table 2. The average deviation in powered flight time for these four flights was only 1.4%. This excellent agreement lends credibility to both the propulsion and aerodynamic ground test programs and to their corresponding performance prediction models.

Flight-to-Ground Data Correlation

Since overall vehicle performance is the combined product of both propulsion and aerodynamic forces, an attempt was made to segregate the propulsion performance characteristics on a system and subsystem level. Flight-to-ground data correlation was conducted for the component performance parameters by comparing delivered values with the ground test data base at steady-state flight conditions. Steady-state regions were defined as those portions of the flight where vehicle flight conditions and ramjet fuel flow settings were either constant or slowly varying.

The correlation process for ramjet thrust was carried one step further than for the subsystem parameters; delivered and predicted levels were compared on a point-by-point basis throughout each of the flights. Predicted thrust levels were obtained by using the vehicle velocity, altitude, and angles of attack measured by the inertial navigation unit; balloon measured atmospheric properties; and fuel flow rate measured by a turbine flowmeter. These were combined with the inlet and ramburner component performance levels obtained during the ground test program to predict thrust.

Delivered performance levels were computed by a variety of techniques that made use of all available flight instrumentation. A summary of these analytical techniques is presented later in this paper; performance results are summarized in this section.

Ramjet Net Thrust

Summaries of ramjet net thrust history for the three primary PTV trajectories are shown in Fig. 4. The thrust values were normalized by ratioing to the predicted thrust at the low altitude takeover condition. The excellent correlation of predicted and delivered thrust shown for these flights is typical of all seven flights. A summary is given in Table 3

showing the standard deviation of the difference between predicted and delivered thrust for each flight, and for the combination of all flights. Ramjet gross thrust was used as the reference base for this error computation since net thrust sometimes passes through zero and this would produce an infinite error. The total standard deviation in thrust performance for all seven flights was only 4.2%.

As shown in Fig. 4, there were only two noteworthy regions with a significant deviation in thrust level. The first region is the initial few seconds of ramjet operation, where delivered thrust is consistently higher than predicted. This phenomena is explained in greater detail in a later section on rocket-to-ramjet transition. The second region occurred on flight 6 during the lean limit descent to a lower Mach number and altitude (time 16-30 s). At the lean limit condition, combustion efficiency falls off rapidly and a considerable deviation could easily be obtained, resulting in a variance in thrust. This will be more evident in the discussion on combustion efficiency.

The divergence at the end of flights 6 and 7 occurred during power-off at very low Mach numbers when the nozzle was no longer filled. This was never added to the prediction because it was anticipated that the missiles would lose control before reaching this condition. The correlation of delivered and ground test predicted thrust was excellent for each of the flights during the cruise and vehicle acceleration regions.

Power-Off Thrust

Figure 5 illustrates the typical thrust performance characteristics obtained during the power-off region at the end of the trajectory. Predicted thrust is presented along with delivered thrust as computed by both the inertial navigation unit and by the air transport duct pressure ($P_{1.7}$). Delivered thrust was initially much higher than predicted. This resulted from heat in the combustor walls combined with the erosion of the char layer on the surface of the thermal protection liner at shutdown. The thrust computed by the duct pressure does not initially reflect the true delivered thrust since the air is choked through the aerogrid, and duct pressure is unaffected by the mass/heat addition in the combustor. This effect dissipates and all three thrust levels eventually converge.

Inlet Performance

The measured flight performance characteristics for inlet mass capture and critical pressure recovery are summarized in Figs. 6 and 7. Subscale wind tunnel test results are also included for relative comparison. The correlation between flight and ground test data was very good. Since inlet mass capture is one of the more critical performance parameters, this correlation with prediction was a significant contribution to the overall success of the flight-to-ground data correlation program.

Burner Pressure Recovery

The derived burner pressure recovery data for all seven flights are summarized in Fig. 8. Data were selected from both power-on and power-off regions. The ground test data base derived from direct connect testing is also presented in Fig. 8. The data correlation was very good; the flight results were within 2% of the ground test results.

Ramburner Combustion Efficiencies

Computed combustion efficiency levels are summarized in Fig. 9. The efficiencies were arbitrarily selected from steady-state regions throughout each of the flights. The band of combustion efficiencies obtained during the direct connect performance documentation testing is also shown.

Combustion efficiencies were typically over 90% in the region of F/A ratios between 0.03 and 0.05. The PTV vehicle cruised in this F/A region for all flight conditions. At lower F/A ratios, a large scatter of combustion efficiencies occurs as in ground testing. Efficiencies dropped off at F/A ratios above 0.05 and then increased again above the stoichiometric value (0.072).

Ramjet Specific Impulse

Ramjet specific impulse levels were evaluated at the steady-state cruise conditions of both high and low altitudes. A statistical average was made and the delivered specific impulse was found to be within 3% of predicted levels.

Rocket-to-Ramjet Transition

The most critical point in the flight of an IRR missile system is the ramjet takeover. If sufficient ramjet thrust cannot be achieved to overcome drag, then the entire mission is lost. Since this is critical, the results obtained during the rocket-to-ramjet transition process deserve some special attention.

A series of interesting and unexpected performance characteristics were encountered during transition on all seven flights. To ensure ramjet takeover under all off-nominal circumstances, PTV was designed with ample margins in both ramjet thrust and inlet supercritical operation. These margins contributed to a totally successful flight test program. When future systems are designed, much of this takeover margin

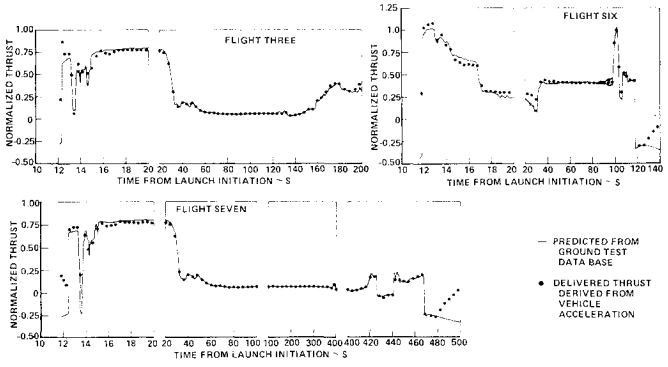

Fig. 4 Ramjet thrust history for primary trajectories.

Table 3 Summary of thrust deviation from prediction

Flight	Standard deviation summary, Delivered vs predicted, %
1	1.52
2	1.57
3	5.43
4	5.74
5	5.76
6	3.02
7	2.71
All flights	4.15

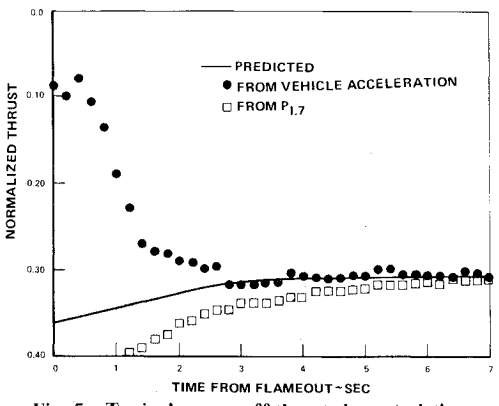

Fig. 5 Typical power-off thrust characteristics.

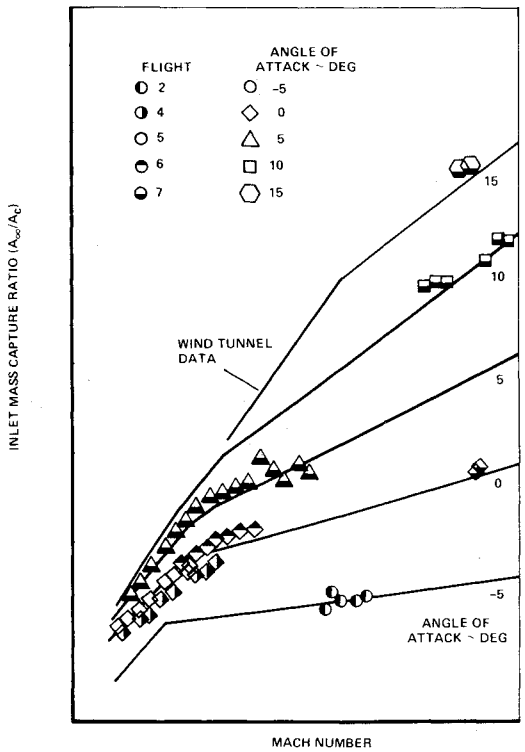

Fig. 6 Inlet mass capture performance.

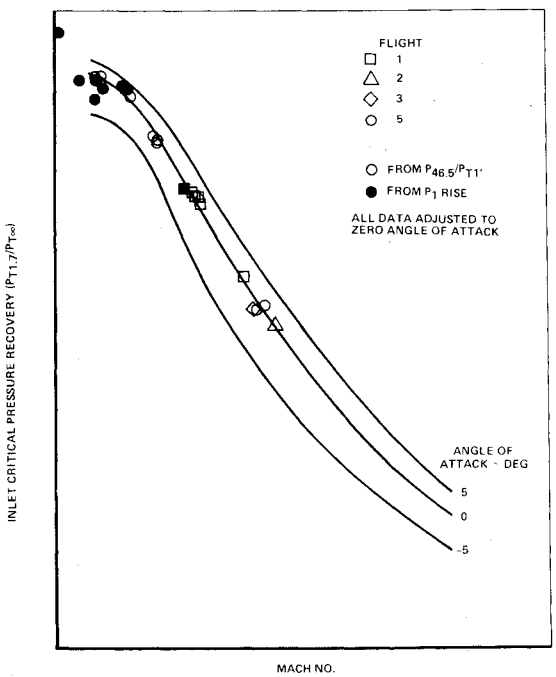

Fig. 7 Inlet critical pressure recovery characteristics.

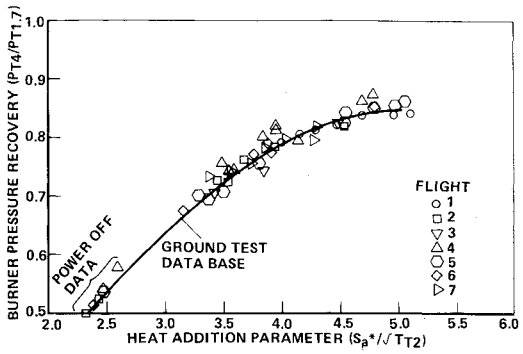

Fig. 8 Burner pressure recovery summary.

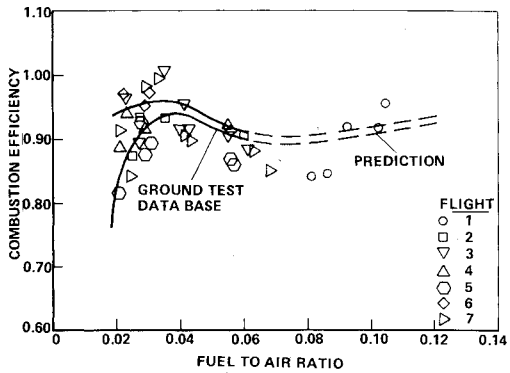

Fig. 9 Ramburner combustion efficiency summary.

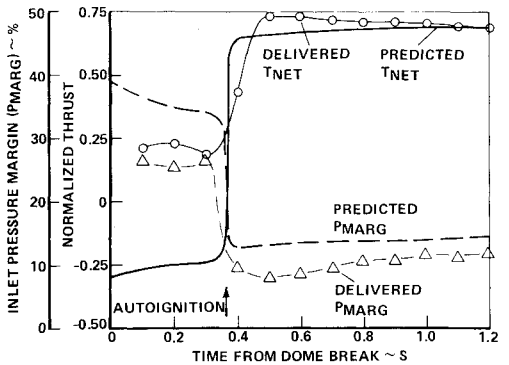

Fig. 10 Typical ramjet performance characteristics during transition.

may be traded for greater range capability. It is essential that an understanding of the PTV transition behavior and its application to future designs be developed.

To avoid potential problems on PTV with a known FMS overshoot and undershoot during startup, the firing of the ramjet flare ignitor was delayed about 1 s; however, during each of the seven flights, the ramburner autoignited as fuel was introduced into the combustor well before the flare was lit. This unexpected autoignition resulted in about 1 s of ramjet operation at fuel flow rates much higher than planned. This was the first contributor to the unusual transition characteristics.

Typical performance characteristics during transition are illustrated in Fig. 10. Delivered and predicted levels of thrust and inlet pressure margin are presented. The predicted values account for the high fuel flow rate due to the FMS overshoot. Thrust levels start higher than prediction and inlet pressure margin begins lower than prediction at ramjet ignition. After a few seconds, the delivered and predicted levels converge. This transient phenomena is typical of all seven flights.

Thrust Characteristics

A summary of the thrust performance levels during transition for each of the flights is presented in Table 4. A comparison of delivered and predicted thrust levels is given for the cold flow region before ignition and the power-on region after ignition. During the power-on region, delivered thrust was repeatedly higher than prediction. The effect is even more dramatic during the cold flow region. Instead of producing negative thrust as predicted, the ramjet produced sufficient positive thrust in this power-off region to accelerate the vehicle.

Potential contributors to a change in thrust are summarized in Table 5. The first five of these can be quickly eliminated since they cannot produce thrust increases of the magnitude given in Table 4, either singularly or in combination. The remaining two parameters, which would be the result of

Table 4 Thrust performance summary during transition

Flight	Normalized cold flow thrust: Post flight prediction	Normalized cold flow thrust: Delivered	Ignition thrust (% increase over prediction)
1	−0.146	+0.231	25
2	−0.239	+0.215	21
3	−0.260	+0.213	37
4	−0.254	+0.135	11
5	−0.273	+0.225	11
6	−0.413	+0.294	6
7	−0.269	+0.170	6

Table 5 Potential contributors to thrust increase during transition

Parameter	Comments
Inlet mass capture	Consistent with prediction[a]
Combustion efficiency	Cannot produce thrust magnitudes[a]
Nozzle efficiency	Cannot produce thrust magnitudes[a]
Fuel heat of combustion	Tested for all flights[a] Would be present throughout all of flight[a] Integrated flow consistent with total fuel[a]
Measured fuel flow	Effect present with no fuel flow[a]
Combustor mass addition	Booster liner and floaters being ejected during transition[b]
Combustor heat addition	Booster liner and floaters burning[b] Heat contained within ramburner walls[b]

[a]Refutes parameter as potential cause. [b]Supports parameters as potential cause.

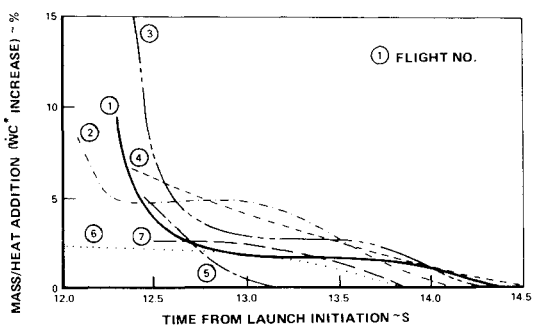

Fig. 11 Ramburner mass/heat addition during transition.

booster residuals, are considered to be the primary contributors to the high thrust levels and probably also caused the fuel autoignition.

An analysis was conducted to determine the amount of mass and heat addition necessary to account for the delivered thrust levels. The results are summarized in Fig. 11. There is a variation in magnitude among the flights, but the typical result is approximately a 7% mass/heat addition at ignition. This effect dissipates after about 2 s. The largest contribution occurred on flight 3, which was the result of a booster propellant sliver that was caused by a known void in the grain. The lowest effect was for flight 6 (low altitude transition). This would be expected: since inlet airflow was much higher, the near-fixed mass/heat addition contribution would have a smaller percentage effect on the ramburner. In addition, the higher combustor shear loads would remove more of the booster residuals prior to ignition.

Inlet Pressure Margin Characteristics

The inlet pressure margin conditions for each ramjet takeover are summarized in Table 6. There are two predictions listed in the table: the first is based on the ground test data base, while the second accounts for the mass/heat addition necessary to match thrust. The actual margins were computed from the transport duct pressure (P_{t7}). The actual inlet margins are less for each flight than the predicted levels. The ramburner mass/heat addition which contributed to higher thrust would also cause a reduction in inlet pressure margin. When this effect is accounted for, the delivered values are usually within 2% of prediction.

Although a 2% agreement on inlet pressure margin was achieved by accounting for the booster residuals, Table 6 indicates that the actual margin is still lower than the prediction. Figure 12 illustrates the computed burner pressure recovery history during transition. During the power-off region before ignition, there is a considerable drop in burner pressure recovery. This effect rapidly dissipates; however, the pressure recovery is still slightly low at ignition. Booster residuals would not contribute to a change in burner pressure recovery, so another contributor had to be found. It was deduced that the most likely cause would be the frangible glass dome. Although an annulus of glass remains bonded to the dome seat after detonation, it was anticipated that the airflow would quickly remove the glass. An investigation of burner pressure recovery data on other ramburner test programs indicates that the change in dump ratio (dump area/combustor area) due to the ¼-in. annulus of glass can produce a change in the burner pressure recovery of the magnitudes indicated. The conclusion is that the frangible glass dome takes several seconds to be completely removed, and this contributes to about a 2% reduction in inlet pressure margin at ramjet takeover. This effect is approximately the same for all takeover altitudes.

Summary of Takeover Characteristics

A summary of the ramjet performance at the various takeover conditions is presented in Fig. 13. Actual and predicted inlet pressure margins are plotted vs the ramjet takeover altitude. The flight results indicate that the lower the takeover altitude, and thus the higher the airflow rate, the closer actual levels will be to prediction. Extrapolation of the data indicates that the PTV vehicle could have been launched at sea level and still successfully transitioned without driving the inlet into subcritical operation.

The PTV vehicle was designed with considerable ramjet takeover margins to ensure that it could withstand unexpected results such as the booster residuals. When designing future IRR systems, these margins would probably be reduced to a minimum to maximize overall vehicle range capability. The results of flight test programs, such as PTV, should be investigated carefully to establish these minimum margins. Consideration should also be given to the potential operation of the inlet in its subcritical region. During the PTV fifth flight, the vehicle was deliberately accelerated from a very low Mach number, with the inlet operating subcritically, to demonstrate stable operation in this region.

Flight Performance Analysis Techniques

During the PTV flight analysis program, a variety of techniques were used to evaluate the propulsion system. Each technique was evaluated to determine the best methods for assessing flight performance. The major techniques are summarized in Table 7, and the physical locations of the instruments are illustrated in Fig. 14. An assessment of the accuracy and reliability obtained on PTV is given in Table 7, as well as an assessment of its potential for future programs.

Table 6 Inlet pressure margin summary during transition

Flight	Inlet pressure margin, %		
	Postflight prediction	Measured by $P_{1.7}$	Prediction assuming mass/heat addition
1	0.5	−3.9	−1.2
2	15.1	4.5	7.5
3	13.6	2.3	2.5
4	14.5	8.7	11.1
5	13.2	7.8	9.6
6	8.7	5.6	6.4
7	15.1	8.4	12.6

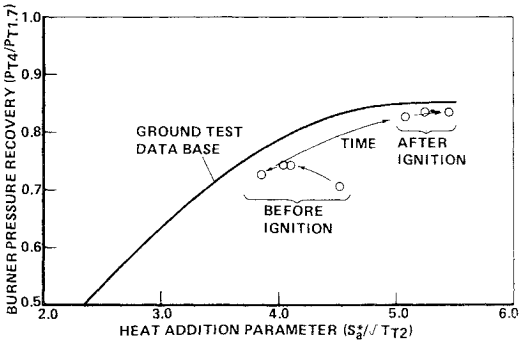

Fig. 12 Typical burner pressure recovery history during transition.

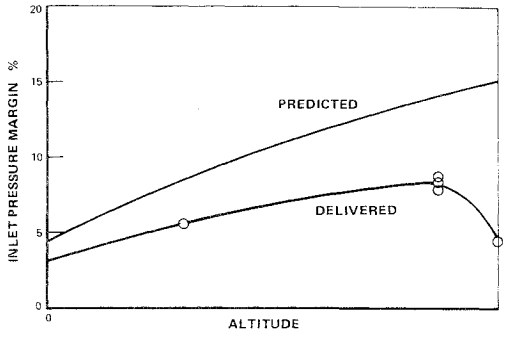

Fig. 13 Effect of altitude on ramjet takeover.

Inertial Navigation Unit

The inertial navigation unit (INU) used for autopilot control evolved as the primary instrument for evaluating propulsion system performance. Vehicle axial acceleration could be derived from the INU for use in establishing the net axial force on the missile. Since this force included the vehicle aerodynamics, external drag was segregated by assuming that it was equal to the results obtained in wind tunnel testing. Body coefficients were separated from those of the air vane, and measured vane position was used to compute drag throughout the flight. Net ramjet thrust was then computed as

$$T_{\text{net}} = m\dot{V}_X + D_{\text{body}} + D_{\text{vane}} \tag{1}$$

This method was intended to be an iterative process since external aerodynamics were assumed to compute thrust. Thrust performance was to be reevaluated as drag estimates were revised. This iteration was unnecessary. Throughout the flights, and most especially during the ramjet power-off regions, aerodynamic force levels were assessed to be within 3% of the wind tunnel test data.

In addition to ramjet net thrust, the INU can be used to compute subsystem parameters. Gross thrust is first obtained by adding the inlet ram drag to the net thrust. Combustor total pressure can then be derived.

$$T_{\text{gross}} = T_{\text{net}} + (\dot{W}_\infty V_\infty / g)\cos(\alpha) \tag{2}$$

$$P_{T4} = T_{\text{gross}} + \frac{P_\infty A_6}{A_5 C_{F_{\text{id}}}\,\eta_{\text{noz}}} \tag{3}$$

The ramburner charcteristic velocity and then combustion efficiency can be computed by

$$C^* = \frac{P_{T4} A_5 g}{\dot{W}_2 + \dot{W}_F} \tag{4}$$

$$\eta_C = \frac{(T_{T2} + \Delta T_{\text{id}})\,(C^*/C^*_{\text{id}})^2 - T_{T2}}{\Delta T_{\text{id}}} \tag{5}$$

Combustor total pressure can also be combined with a measured transport duct pressure to compute the burner pressure recovery.

Owing to the reliability of the external aerodynamics ground test program and the accuracy of the INU, this performance analysis technique proved to be an excellent method for PTV. This technique was consistently reliable throughout each of the flights, and proved effective during steady-state and transient conditions. The performance results presented earlier for thrust, burner recovery, and combustion efficiency were derived from the INU.

This technique is recommended on future flight test programs as a result of the success obtained on PTV using the INU; however, the sophistication of this system may not be needed for guidance, or justifiable for use solely as a data analysis system. For missile systems having an INU onboard, this technique should definitely be used to assess performance. When this is not available, one of the following pressure measurement techniques, with some qualifications, should be considered for cost effectiveness.

Combustor Pressure

The combustor static pressure (P_4) was the preflight selection as the primary means of computing thrust, combustion efficiency, and burner pressure recovery. The air specific impulse at the throat is first computed using the relationship shown in Fig. 15. This relationship was derived from the results of direct connect testing. Combustor total pressure is then computed.

$$P_{T4} = S_a^* \dot{W}_2 / A_5 C_F \tag{6}$$

Ramburner gross thrust, and in turn ramjet net thrust, can be derived with the relationships already shown in Eqs. (3) and (2), respectively. Combustion efficiency and burner pressure recovery can also be determined using the same relationships shown for the INU.

This technique proved to be unreliable for PTV owing to instrumentation difficulties. During the initial portions of flight, the P_4 measurements produced reasonable results, but subsequent transducer readings drifted considerably. Typical results are shown in Fig. 16, where two transducers

Table 7 Propulsion system flight data analysis techniques

Measurement	Description	Computed performance parameters	PTV results	Recommendations
Inertial navigation unit (INU)	INU velocity components	Thrust Combustion efficiency Burner pressure recovery (in conjunction with $P_{1.7}$)	Excellent reliability on all flights	Highly recommended
P_4	Combustor static pressure	Thrust Combustion efficiency Burner pressure recovery (in conjunction with $P_{1.7}$)	Experienced significant thermal drift	Shows potential—needs further investigation
$P_{1.7}$	Transport duct static pressure	Thrust Combustion efficiency Inlet pressure margin Burner pressure recovery pressure (in conjunction with P_4 or INU)	Good reliability on all flights	Recommended
P_3	Combustor forward dome pressure	Thrust Combustion efficiency Burner pressure recovery (in conjunction with $P_{1.7}$)	Sluggish response due to greased line; fair results during steady state	Potential backup
$P_{46.5}$	Inlet diffuser static pressure	Thrust Combustion efficiency Inlet pressure margin	Good results during near critical conditions	Limited backup

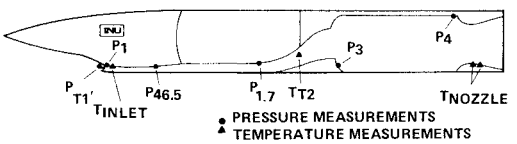

Fig. 14 Major propulsion system instrumentation localities.

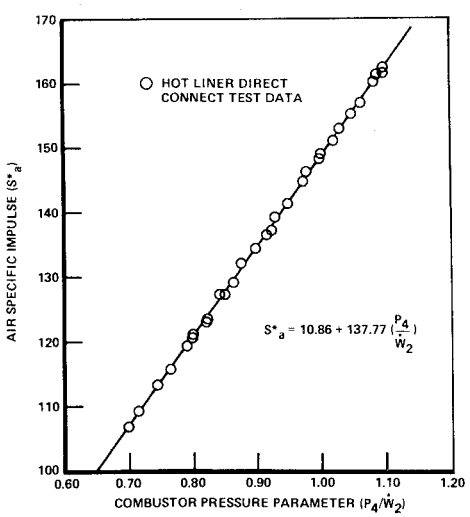

Fig. 15 Air specific impulse relationship.

manifolded to a common pressure tap are compared to predicted levels. This particular data are for the powered dive portion of flight 3. The transducer diaphragms were locally heated by the hot combustor gases, causing a large offset in the calibration of the transducers. This problem was discovered during ground testing, and the transducer cavities were filled with grease to thermally isolate them. Though this effort delayed the problem, the transducers continued to drift.

The P_4 measurement is still believed to be a good thermodynamic means of evaluating propulsion performance, and it is recommended that this means be considered for future systems. However, further developmental work will be

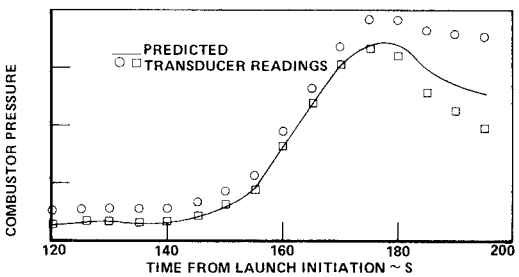

Fig. 16 Typical performance drift with combustor pressure transducers.

needed to ensure that selected pressure transducers can withstand the 4000 + °R combustor temperatures and still be able to maintain reasonable response characteristics to assess dynamic behavior in the combustor.

Transport Duct Pressure

The transport duct static pressure ($P_{1.7}$) can be used to mass derive the duct total pressure using the following relationship:

$$\frac{\dot{W}_{1.7}}{A_{1.7}} = \sqrt{\frac{\gamma g}{RT_{T2}}\left(1+\frac{\gamma-1}{2}M_D^2\right)}\,(P_{1.7}M_D) \qquad (7)$$

The total pressure can be obtained using the isentropic relationship after solving for the duct Mach number. The relationship shown in Fig. 17, which was derived from the ground test burner pressure recovery data, can then be used to derive combustor total pressure. The computation of thrust and combustion efficiency follows the same method shown for the P_4 measurement. To compute burner pressure recovery, the duct total pressure must be combined with another means of determining combustor total pressure. The duct pressure is also used to assess inlet pressure margin by comparing it to the critical pressure recovery levels obtained in wind tunnel testing. $P_{1.7}$ also served as the primary means for computing airflow rate. This could be accomplished during the power-off region by determining the airflow through the choked aerogrid.

This method was used successfully on the PTV program. The instrumentation did not experience the same thermal drift as the combustor pressure transducers did owing to the lower air temperatures in the duct and the relatively long tubing leading to the transducer.

This method's basic deficiency during PTV was instrumentation accuracy at the low pressures experienced at high altitude conditions. Nevertheless, a duct pressure measurement will be essential for future flight test programs; the airflow measurement capability alone will justify it. It is also a valuable tool for computing burner pressure recovery, inlet pressure margin, and thrust levels. A more judicial selection of multirange transducers should be considered to avoid the accuracy problem.

Combustor Forward Dome Pressure

The combustor forward dome pressure (P_3) can be used to derive the combustor static pressure (P_4) by means of the relationship shown in Fig. 18. This relationship was derived from the results of freejet testing. Once P_4 is obtained, performance parameters can be derived using the same techniques mentioned earlier for the combustor pressure.

However, owing to the recirculation zone caused by the sudden dump, P_3 was considered to be a nonviable method for computing performance. Also, the tubing leading to the transducer was completely filled with grease to protect it during the booster operation. This resulted in a very sluggish response to pressure changes during ramjet operation.

Results obtained during PTV indicated some potential for the P_3 measurement. Although nonresponsive to changing conditions, the computed thrust levels from P_3 approached actual levels during long steady-state conditions. The P_3 measurement would not be recommended as a means of primary performance computation, but could be considered as a backup method when refined.

Inlet Diffuser Pressure

By using the relationship shown in Fig. 19, the transport duct pressure can be derived from the diffuser static pressure ($P_{46.5}$). This relationship was derived from wind tunnel test data. Performance parameters can then be computed using the methods mentioned earlier for the duct pressure. This method can be used only at low inlet supercritical conditions where the shock train is forward of the pressure tap and the flow aft of the tap is subsonic. Performance calculations using $P_{46.5}$ were fairly reliable. Although useful as a backup technique, this method unfortunately was applicable less than 10% of the flight time.

Miscellaneous Performance Parameters

In addition to the major analysis techniques already mentioned, there are a number of parameters which had to be appropriately treated to produce a reasonable accuracy for both delivered and predicted performance levels. Owing to the high PTV speeds, the derivations of freestream total pressure and temperature were adjusted for real gas effects. Isentropic solutions would have produced temperature errors of over 100 °R. Knowing the temperature of the air dumping into the combustor is essential since a considerable amount of heat is lost into the forebody structure. This was accomplished by using total temperature probes just upstream of the dump.

The fuel flow rate was a critical parameter for performance computations. To ensure accurate measurements on PTV, a Hoffer turbine flowmeter was installed. A comparison of integrated fuel flow and total fuel loading indicates that measurements were correct to within 1%.

The airflow rate was also a very critical parameter, but could only be determined during the power-off regions at the end of the trajectory when the temperature of the airflow through the combustor would be known. Figure 20 summarizes two relationships for computing airflow through the choked aerogrid using $P_{1.7}$, and through the choked ramjet nozzle using P_4. Direct connect data and freejet test data were used to assemble these relationships. A special fuel cutoff was added to flight 7 during the dive portion at high supersonic conditions since the power-off conditions for the first six flights all occurred at low Mach numbers and altitudes. After

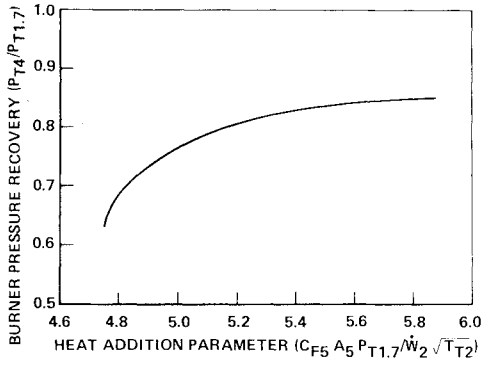

Fig. 17 Combustor pressure relation using duct pressure.

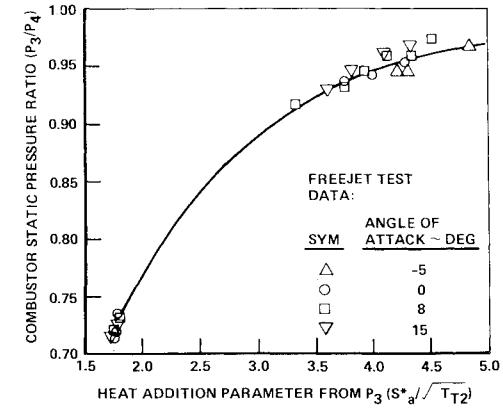

Fig. 18 Combustor pressure relation using forward dome pressure.

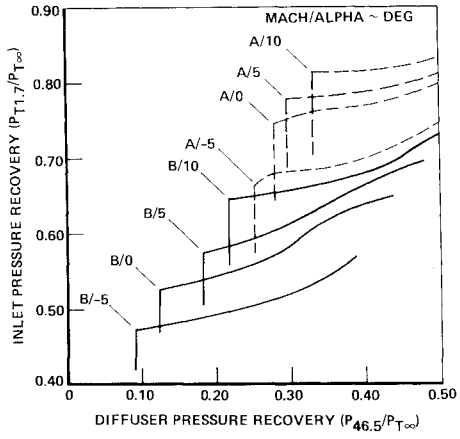

Fig. 19 Duct pressure relation using diffuser pressure.

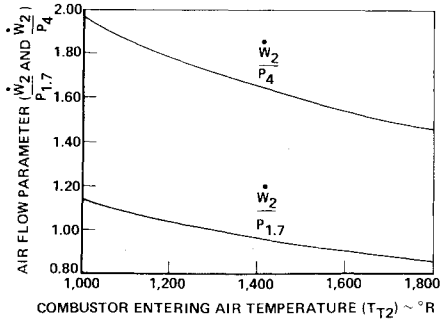

Fig. 20 Airflow relationships.

obtaining mass capture data, fuel flow was reinitiated, the engine autoignited, and the powered flight was continued. The $P_{1.7}$ method served as a primary means of computing airflow. The P_4 instrumentation drift invalidated the other method.

In the initial stages of the PTV flight program there was no plan to obtain inlet critical pressure recovery data since the selected flight profiles would not cause subcritical operation. Owing to the success attained on the first four flights, the fifth flight was altered to specifically investigate inlet performance. The flight consisted of a series of decelerations to and accelerations from steadily decreasing Mach numbers. The inlet was driven into subcritical operation on the last two velocity excursions, and then passed back into supercritical operation as the vehicle accelerated to a higher speed. Figure 21 illustrates how the inlet face static pressure (P_1) was used to assess the operation of the inlet as it passed through its critical stage. As the normal shock passes out of the inlet, it causes a rise in P_1. The pressure then drops back to its normal supercritical level when the shock moves back into the inlet. Once the critical points have been identified, the transport duct pressure ($P_{1.7}$) can then be used to compute the critical pressure recovery.

A secondary method for computing critical pressure recovery was also evaluated. The flight values for the ratio of diffuser pressure to inlet face pitot pressure ($P_{46.5}/P_{T1'}$) were compared to the pressure margin relationships obtained in the subscale wind tunnel testing, as illustrated in Fig. 22. The estimated inlet pressure margin was combined with the actual pressure recovery obtained with $P_{1.7}$ to calculate critical pressure recovery,

$$\left(\frac{P_{T1.7}}{P_{T\infty}}\right)_{crit} = \frac{(P_{T1.7}/P_{T\infty})}{(1-P_{\text{marg}}/100)} \tag{8}$$

The results obtained with these two techniques were presented in Fig. 7, with the agreement between flight and ground testing being very good.

Two key physical parameters, inlet capture area and nozzle throat area, were time dependent, varying with the flight conditions. The inlet growth factors shown in Fig. 23 were derived from a finite-element analysis to establish the inlet growth as a function of local pressure and temperature. Flight measurements were then used to assess actual inlet size throughout the flights. Nozzle throat area reduces as the silica phenolic nozzle insulation heats and swells, since the insulation is constrained from outward growth by the Inconel shell. Postflight measurements and ground test measurements were used to derive the relationship between nozzle throat area and structure temperature shown in Fig. 24. A flight temperature measurement was used with this relation to assess end-of-flight nozzle throat area. Since there is a considerable time lag before heat passes through the nozzle insulation to the shell, the throat experiences a considerable change before the shell temperature changes. Thus Fig. 24 cannot be used to assess throat area in the early portions of the flight. Instead, this relationship is used only to identify the throat area at the end of flight. Direct connect data were evaluated, and it was determined that the throat area would follow an exponential curve from the initial to the final area with an exponent of 0.35.

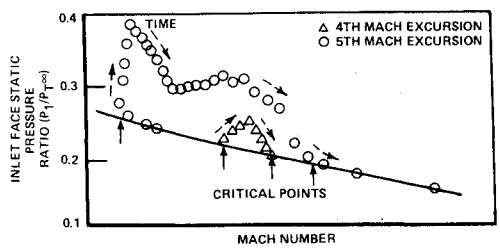

Fig. 21 Evaluation of inlet critical points.

Ground Test Program

Performance characteristics were documented for each of the propulsion system components during the PTV ground test program. A proper understanding of all performance parameters is required to accurately predict flight performance. Figure 25 gives a summary of the PTV ground test program and illustrates which tests were used to establish a data base for inlet mass capture, inlet critical pressure recovery, burner pressure recovery, combustion efficiency, and nozzle efficiency. These five component parameters, when combined with the flight conditions and fuel settings, were used to predict ramjet thrust and inlet pressure margin.

Inlet mass capture and critical pressure recovery data used for flight prediction were taken from the 0.4 scale inlet wind tunnel test. Although higher mass captures were obtained in freejet testing, it was felt prior to flight that the wind tunnel data would best represent expected flight results. This assumption proved to be correct.

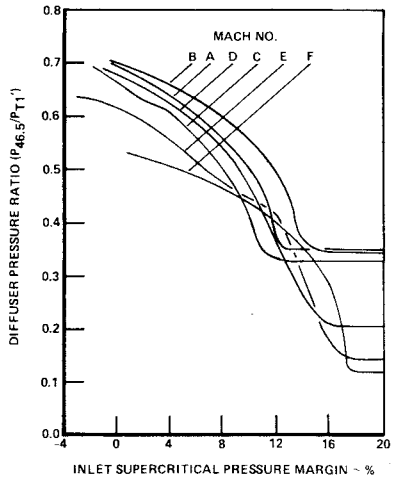

Fig. 22 Pressure margin relationships to pressure.

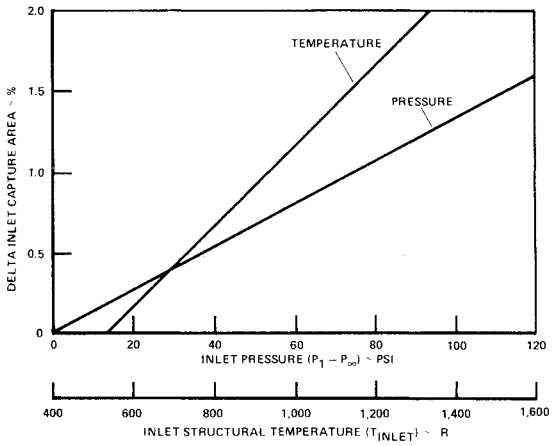

Fig. 23 Inlet growth factors.

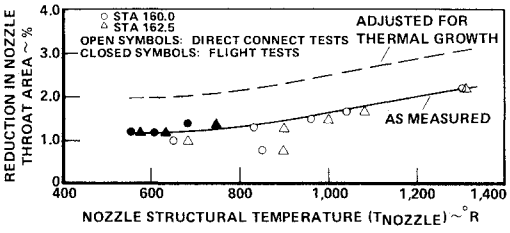

Fig. 24 Nozzle throat area change relationship.

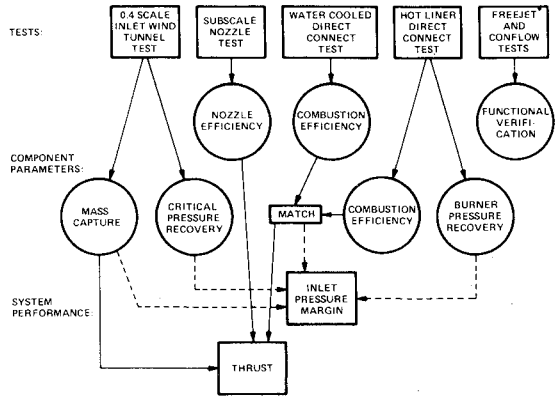

Fig. 25 Ground test performance documentation program.

Combustion efficiency levels used in the prediction data base were taken from water-cooled direct connect testing. This type of testing allowed for rapid and efficient testing at many flight conditions while maintaining a consistency among test runs since thermal transients were minimized. Combustion efficiency levels were then verified in select hot liner direct connect tests.

Burner pressure recovery data were taken from the hot liner tests. Recoveries during this series were almost 2% higher than those obtained during water cooled testing. Although combustion efficiencies can be easily adjusted for heat losses into the water cooled chamber, the effect on pressure recovery is more difficult to assess. Hot-walled testing proved to be more representative of expected flight results.

The excellent correlation between flight test results and predictions derived from ground testing is the best evidence supporting the PTV performance documentation ground testing. This proves conclusively that a ground test program can adequately predict flight performance for a ramjet propulsion system.

Much of the success attained on PTV can be attributed to its ramburner design. Relatively constant combustion efficiencies were obtained over a broad range of flight conditions. PTV was a very stable running engine with no evidence of any combustion instabilities. For different ramburner designs, such as ones with a short length-to-diameter ratio, performance results could vary considerably over its operating envelope. Results obtained in hot-walled testing should be matched carefully with the results of water cooled testing in future programs. Discrepancies should be evaluated and decisions should be made concerning the amount of hot-walled testing necessary to document performance.

In addition, live rocket-to-ramjet transition should be conducted over the full range of potential launch altitudes. Since most systems will not have the ramjet takeover margins that were designed into PTV, it is important that the effects of the booster on ramjet takeover be appropriately identified. This identification should be made at altitudes other than the low altitude launch since trends indicate (Fig. 13) that inlet margins could be less at higher altitudes. Freejet transition testing should be seriously considered so as to identify the characteristics of the entire propulsion system.

Summary and Conclusions

All PTV performance evaluation objectives were accomplished during the flight test program. Various performance analysis techniques were assessed during the program, and new methods were found to evaluate a ramjet system in flight. The correlation between flight performance results and predictions based on ground testing was found to be excellent. Those results gave credence to the PTV ground test program, and proved that a ground test program can accurately predict flight performance.

Overall system performance and subsystem performance levels were close to prediction throughout all flights. Flight times to fuel depletion were within 2% of preflight predictions. Computed thrust levels throughout all the trajectories had a standard deviation of 4% compared to predictions based on the ground test data base.

Valuable information was learned during the rocket-to-ramjet transitions concerning ramjet takeover performance characteristics. The effects of booster residuals for PTV were also distinctly quantified. Demonstrated operation in the inlet subcritical region served to verify that a ramjet system with a chin inlet can use this region for design margins.

The PTV test program has produced a wealth of test data from which required performance margins can be reassessed. Future designs of IRR systems can use the PTV flight test results to ensure that the systems will have optimized performance capabilities and reliable margins.